ELSEVIER

Biochimica et Biophysica Acta 1233 (1995) 68–74

BBA Biochimica et Biophysica Acta

Real-time X-ray diffraction study at different scan rates of phase transitions for dipalmitoylphosphatidylcholine in KSCN

B.A. Cunningham [a,*], P.J. Quinn [b], D.H. Wolfe [c], W. Tamura-Lis [d], L.J. Lis [e], O. Kucuk [e,1], M.P. Westerman [e]

[a] *Department of Physics, Bucknell University, Lewisburg, PA 17837, USA*
[b] *Department of Biochemistry, King's College, London, Campden Hill Road, London W8 7AH, UK*
[c] *Department of Astronomy and Physics, Lycoming College, Williamsport, PA 17701, USA*
[d] *University of Nebraska Medical Center, Omaha, NE 68105, USA*
[e] *Division of Hematology / Oncology, UHS / The Chicago Medical School, The Veterans Affairs Medical Center, N. Chicago, IL 60064 and Mount Sinai Hospital Medical Center, Chicago, IL 60608, USA*

Received 18 May 1994; accepted 26 September 1994

Abstract

Multibilayer arrays of dipalmitoylphosphatidylcholine (DPPC) in 1 M KSCN were characterized using real-time X-ray diffraction and differential scanning calorimetry. A phase transition sequence was observed as a function of increasing temperature which involved changes from the interdigitated subgel (L_c(inter)) to interdigitated gel (L_β(inter)) to disordered (L_α) bilayer states. The phase transition mechanisms were unambiguously determined by comparison of results from fast and slow scans. The L_c(inter) → L_β(inter) phase transition was shown to involve a continuous change in acyl chain spacing between the rectangular subgel acyl chain unit cell into an hexagonal gel acyl chain unit cell. The mechanism is similar to that for subgel to gel state transitions involving non-interdigitated DPPC bilayers.

Keywords: Phospholipid; X-ray diffraction; Interdigitated phase; Lipid phase behavior

1. Introduction

The interdigitated bilayer phase has been shown to occur for at least one phospholipid in water [1–4], and other phospholipids in aqueous systems containing a variety of solutes [4–9] including 1 M KSCN [4,10–13]. We have previously described the phase transition sequence for dipalmitoylphosphatidylcholine (DPPC) in 1 M KSCN using a real-time X-ray diffraction technique [11] when the initial phase in the study was the gel-state interdigitated bilayer phase. However, it has been previously inferred that DPPC in ethanol/water solutions may form interdigitated subgel phase bilayers [4,14], with a resulting dynamic phase transition sequence of L_c(inter) → L_β(inter) → L_α, and that dihexadecylphosphatidylcholine (DHPC) in water also forms interdigitated subgel phase bilayers [2,4], with a resulting equilibrium or dynamic phase sequence of L_c(inter) → L_β(inter) → $P_{\beta'}$ → L_α. It is therefore of interest to determine the phase transition sequence for DPPC in 1 M KSCN as it relates to the aforementioned DPPC in ethanol/water and DHPC in water studies.

Real-time X-ray diffraction [15] has been shown to be useful in determining phase transition mechanisms and thermodynamic order as well as dimensional parameters for the phases studied. An apparent first-order thermodynamic process occurs via the coexistence of initial and final states [16] as indicated by the presence of coexisting diffraction patterns from both states. Higher order transitions [16], being critical phenomena, proceed via the presence of intermediate states that may be from unique phases [17–19] or continuous changes in the structure of the initial state eventually resulting in the formation of the final state [20–22]. Tenchov and co-workers [23] have confirmed that the kinetics of a transition may influence the apparent transition mechanism. Since some transitions

* Corresponding author. Fax: +1 (717) 5243760.
[1] Present address: Cancer Research Center of Hawaii, 1236 Lauhala Street, Honolulu, HI 96813, USA.

SSDI 0005-2736(94)00237-1

may be slow, slow scan rates are required to insure an unambiguous classification. However, such examinations must be done within time periods for X-ray exposure which will minimize radiation damage to the sample [24,25]. Extremely fast transition jumps [26–28] do not lend themselves to the determination of transition mechanisms due to the limitations in detector response which can preclude the recording of diffraction patterns from intermediate states, thus most fast scans can only indicate the presence of coexisting states. In addition, the use of small stepwise or continuous changes in temperature provides the lowest entropic or reversible transition pathway. Of course, it should be noted that the mechanism of a dynamic phase transition cannot be obtained from static or stepwise measurements at different temperatures since the entropies of the two processes would be different [16].

In this report, we have examined the dynamic phase sequence for DPPC in 1 M KSCN starting with an initial subgel phase at two different scan rates. This was done in order to determine the transition mechanism for the L_c(inter) to L_β(inter) transformation, as well as to determine whether the rippled phase is an intermediate between the gel and disordered bilayer phases. The presence of a ripple phase would indicate that the bilayer does not possess any other mechanism by which to dissipate the mechanical stress produced by the thermal expansion of the lipid headgroups [4].

2. Materials and methods

Dipalmitoylphosphatidylcholine was obtained from Avanti Polar Lipids (Alabaster, AL). Salts were reagent grade and the water was distilled. Lipid dispersions for X-ray diffraction were made by mixing known amounts of lipid powder and salt solution, with subsequent heating at ≈ 60°C until all the powder appeared to be hydrated. Samples were stored at ≈ 0°C until examination by X-rays.

Calorimetry was performed using a Perkin-Elmer DSC-2 scanning calorimeter fitted with a subambient accessary and interfaced to an IBM PS/2 with a Metrabyte DAS-16 data acquisition board (Keithley, Tauton, MA). Lipid samples were hydrated by direct addition of 1 M KSCN (1/1, w/w) to the lipid powder at room temperature and hermetically sealed in aluminum pans. All samples were cooled and heated over the range -9°C to 71°C and thermograms were recorded on heating at a rate of 5°C/min after 1–2 days equilibration in the calorimeter at -9°C. Previous studies [10,13] have indicated that slower scan rates do not affect the determination of thermodynamic parameters. Temperature scans were repeated three times. Onset transition temperatures were taken to be the temperature at which the rising endotherm departed from the baseline. Lipid transition parameters were determined by calibration with the known transition temperature and enthalpy for the melting of indium.

X-ray experiments were performed using a monochromatic (0.15 nm) focussed X-ray beam at Station 8.2 of the Daresbury (UK) Synchrotron Laboratory. A purpose built camera allowed clear resolution of reflections between 10 nm and 0.35 nm. The sample holder was a cryostage (Linkam Scientific, Tadworth, UK) to which mica windows were fitted. The sample size was about 15 μl with a path length of 1 mm. The stage was cooled to liquid nitrogen temperature and heated to the required temperature by imbedded heating elements in the stage. Temperature programming over the range -50°C to 200°C at rates between 0.001°C/min to 2.3°C/s were possible. Sample temperature was monitored by a thermocouple imbedded in the cryostage. A temperature gradient of less than 0.5°C existed across the sample and the sample temperature was at most 1°C different than the internal temperature of the cryostage. The samples were cooled in the camera to -50°C and allowed to equilibrate for several minutes until the L_c phase was formed. The L_c phase can also be induced by equilibrating the lipid sample at ≈ 0°C for 1–4 days.

X-ray data were collected using a single wire linear detector fabricated at the Daresbury Laboratory. The samples were subjected to controlled heating scans at rates of 5°C/min or 0.2°C/min between defined temperature limits. The data collection system allowed 255 diffraction patterns to be collected consecutively with a 10 μs wait-time between patterns. The exposure time for each pattern was 3 s for the 5°C/min scan and 10 s for the 0.2°C/min scan. Each temperature scan was repeated twice. The acquired data were stored in a VAX-11/750 computer and corrected for detector response by comparison with a pattern recorded using a fixed source and the spacial calibration was obtained using Teflon [29]. Data were analyzed using the OTOKO program provided by the Daresbury Laboratory which was updated from the original version by Boulin et al. [30]. Figures were produced using Stanford Graphics™ (3-D Visions, Torrence, CA) which allowed for the production of both two- and three-dimensional presentations of the data. Two-dimensional projections were produced using a slice of the intensity in order to show both low and high intensity peaks. Although the two-dimensional representations accurately portray the transitional information in the data set, exact structural parameters cannot necessarily be obtained from the figure. Structural parameters were determined by analyzing each of the 255 individual diffraction patterns in the data set. Uncertainties in the lamellar d-spacings were ± 0.19 nm and in the acyl chain scattering peaks were ± 0.001 nm.

3. Results and discussion

The dynamic phase transition sequence for DPPC in 1 M KSCN has been previously reported for the case where the gel bilayer phase was the starting point of the study

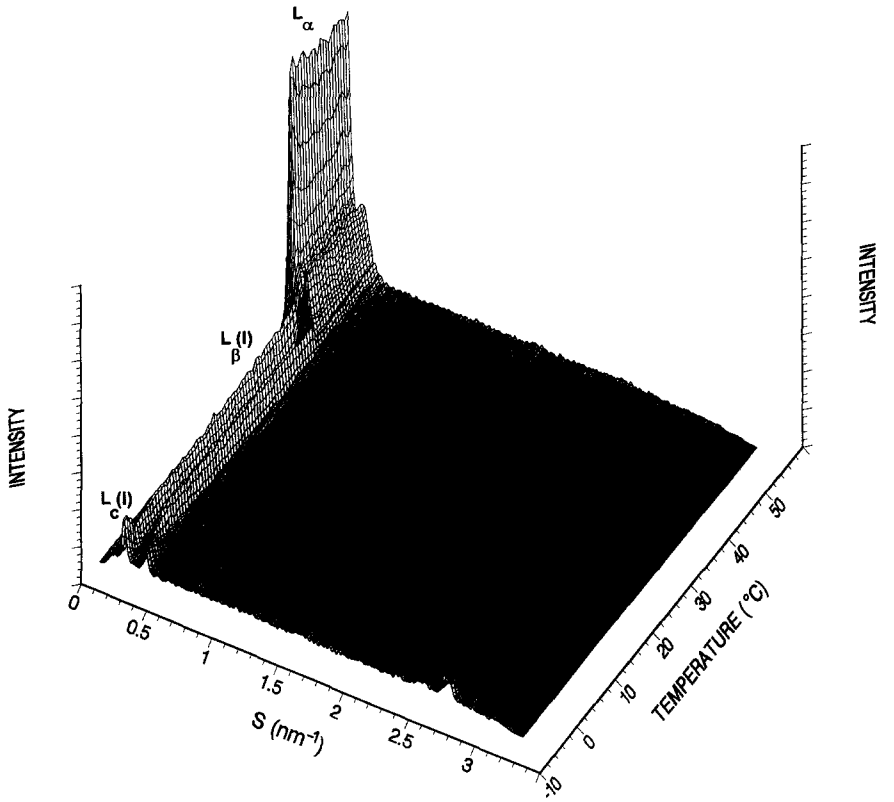

Fig. 1. Three-dimensional plot of scattered intensity versus reciprocal spacing (S) for DPPC in 1 M KSCN undergoing a heating scan of 5°C/min. Every third diffraction pattern of 3 s duration is shown. The interdigitated subgel phase $L_c(I)$, the interdigitated gel phase $L_\beta(I)$, and the disordered bilayer phase L_α are indicated on the figure.

[11]. It has become apparent that the subgel phase is the low temperature equilibrium phase for DPPC bilayers and a more appropriate starting point for studies exploring the temperature induced phases and phase transitions. Fig. 1 shows representative diffraction patterns for a DPPC in 1 M KSCN sample undergoing a 'fast' linear temperature scan of 5°C/min. Both the sub gel and gel phases produce mesophase diffraction peaks with the characteristic low intensity observed with interdigitated phases (see, for example, Ref. 6). The initial phase has a bilayer repeat (d-spacing) of 5.20 nm and the acyl chain scattering produced two wide-angle diffraction peaks at 0.385 and 0.407 nm (see Fig. 2). This lamellar d-spacing is significantly smaller than that observed for DPPC in water (i.e., 6.0 nm) which is an indication that the DPPC bilayers in 1 M KSCN may contain interdigitated acyl chains in the L_c phase. It should be noted that gel state DPPC bilayers in 1 M KSCN equilibrated at 25°C have a bilayer repeat of 5.29 nm and a lipid thickness of 2.77 nm [10]. The L_c(inter) phase assignment is consistent with other lipid systems that form sub gel and gel state interdigitated bilayers [2,14].

The L_c(inter) phase transforms into the previously described L_β(inter) phase at approx. −2.7°C. The L_β(inter) bilayer repeat spacing immediately after the transformation

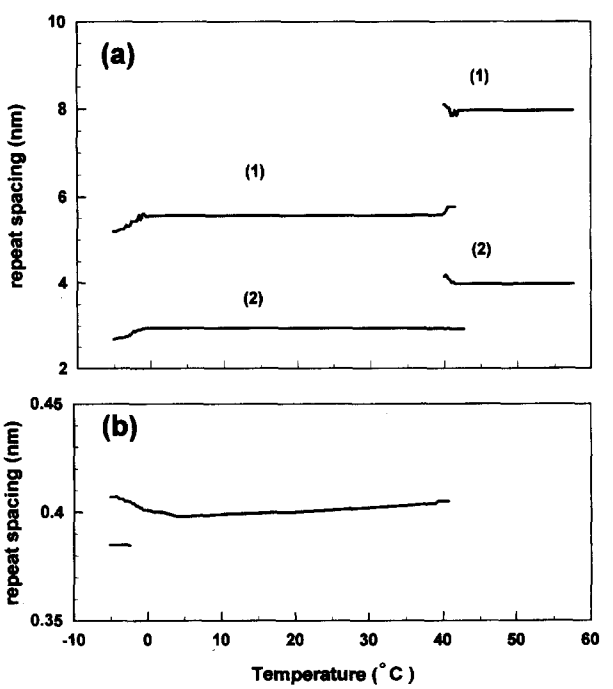

Fig. 2. Repeat spacings of the (a) small- and (b) wide-angle X-ray scattering regions for DPPC in 1 M KSCN as functions of temperature. Numbers in parentheses correspond to the order of a one-dimensional, lamellar lattice.

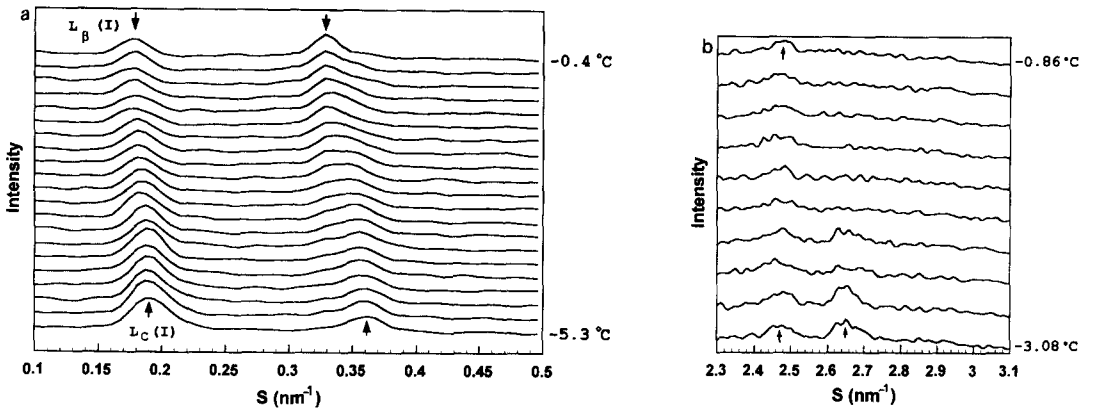

Fig. 3. Typical sets of X-ray diffraction patterns for DPPC in 1 M KSCN showing the L_c(inter) → L_β(inter) phase transition for the (a) small-angle region and (b) wide-angle region. The characteristic diffraction maxima of the L_c(inter) and L_β(inter) phases are indicated by arrows in (a), whereas the position of the diffraction maxima arising from the acyl chains are indicated by arrows in (b).

is 5.66 nm with the hexagonal two-dimensional acyl chain packing at 0.403 nm. The difference between the bilayer repeat spacings obtained using real-time X-ray diffraction (Fig. 1 and 2) and static X-ray diffraction at a specific temperature [4] is due to the dynamics involved with the real-time technique. The samples undergoing a continuous temperature change do not change states by a series of equilibrium states but by transitions involving the smallest changes of enthalpy possible. For lipid systems, the transformations will require longer times for water equilibration across the defect structures throughout the multilamellar array, rather than in changes in lipid packing and bilayer thickness [11,14,17–23]. This speculation is consistent with Cevc's description of the subgel-to-gel phase transition [31] as a loosening of the acyl chain interactions. Such a change in intramembrane interactions would result in greater lipid headgroup areas and therefore an increased headgroup hydration requirement.

The L_c(inter) to L_β(inter) phase transition proceeds (Figs. 2 and 3) via an apparent continuous change in the acyl chain and bilayer dimensions; i.e., a second-order phase transition. This result is consistent with previous studies of other subgel to gel bilayer phase transitions in lipid–solvent systems [2,17,22]. We cannot rule out that our observations were influenced by the mode of L_c phase formation. We can, however, rule out that the phase proceeds by an overlap of the first order diffraction peak of the initial and final phases. This would result in a broadening of the first order diffraction peak as the second phase is nucleated rather than the observed continuous decrease in peak breadth. It is less likely that these studies are influenced by the presence of ice, since no hexagonal ice diffraction peaks were observed [32] and passage of the sample through O°C did not result in a dramatic increase in *d*-spacing as expected when ice melts. Our quick cooling to −50°C may be too short in time to allow for ice formation. Additionally, calorimetry studies of DPPC in 1 M KSCN show two transitions which can be identified as the sub- and main transitions (Fig. 4). The calorimetric parameters are listed in Table 1 for these transitions. The subtransition temperature (Table 1) is in reasonable agreement with the observed L_c(inter) to L_β(inter) phase transition (Fig. 1 and 2) and the main transition temperature and enthalpy agree with previously reported values [10]. We do not observe a large endotherm from the melting of ice. The appearance of a change in specific heat (C_p) with an integrable peak and transition enthalpy (ΔH) is apparently inconsistent with the X-ray data which indicates a second order phase transition mechanism which should have resulted in a change in the slope of C_p with no discernable

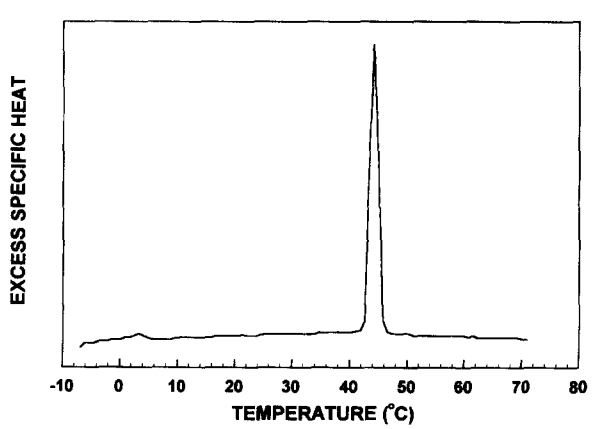

Fig. 4. Differential scanning calorimetry heating curve for DPPC in 1 M KSCN undergoing a heating scan at 5°C/min with a sensitivity of 0.5 mcal/s. The sample was equilibrated at −9°C for 1–2 days in the calorimeter before being scanned.

Table 1
Calorimetric data for the transitions of DPPC in 1 M KSCN

Parameter	Transition	
	Sub	Main
T (K)	−2.3±0.1	39.4±0.1
ΔH (kcal/mol)	0.42±0.05	10.12±0.01

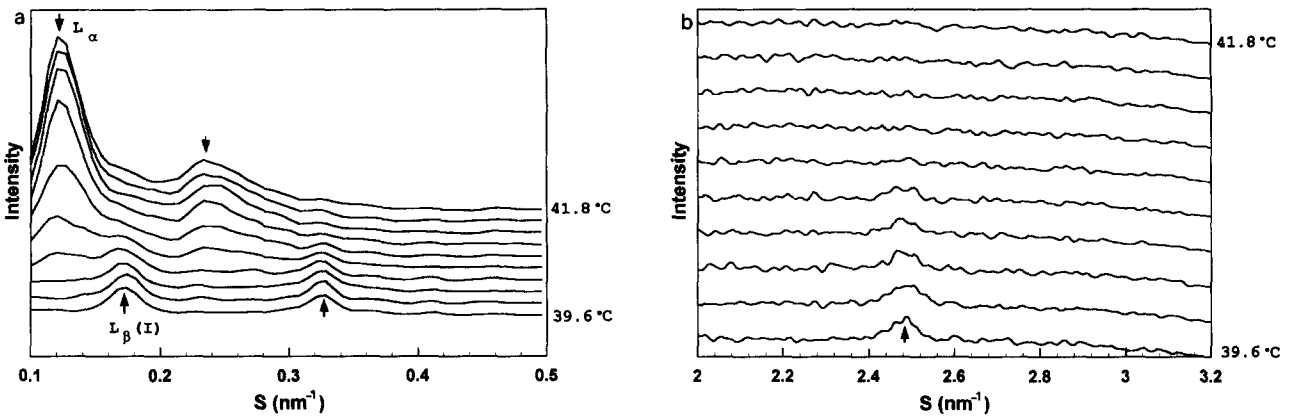

Fig. 5. Typical sets of X-ray diffraction patterns for DPPC in 1 M KSCN showing the L_β(inter) → L_α phase transition for the (a) small-angle region and (b) wide-angle region. The characteristic diffraction maxima of the L_β(inter) and L_α phases are indicated by arrows in (a), whereas the position of the diffraction maxima arising from the acyl chains are indicated by arrows in (b).

ΔH. However, we would expect that the sub gel to gel phase transition would result in lipid molecules with greater energy. A loosening of the acyl chain packing could result in some disordering of the acyl chains [31] and endothermic release of energy. The change in C_p slope would be so small as to have little influence on the calorimetric endotherm shape. Thus, this second order phase transition initiates a secondary release of energy resulting in a calori-

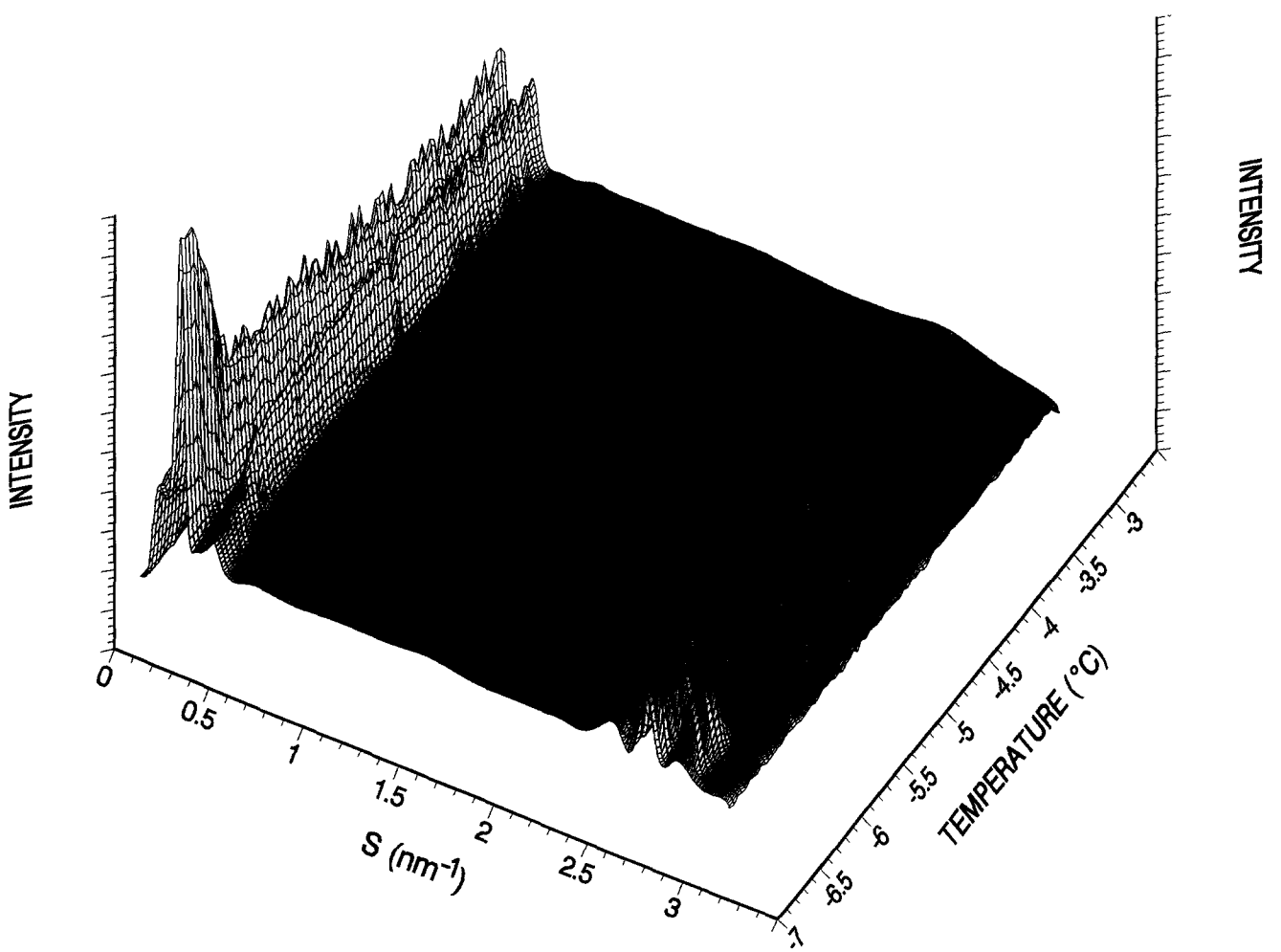

Fig. 6. Three-dimensional plot of scattered intensity versus reciprocal spacing (S) for DPPC in 1 M KSCN undergoing a heating scan of 0.2°C/min. Every third frame of 10 s duration is shown.

metric endothermic peak. This measurable enthalpy for a second order phase transition is also observed in the transition of the L_c to L_β phase for DPPC in water [17] and for the L_c to L_β(inter) phase for dihexadecylphosphatidylcholine [2].

The next observed phase transition occurred between the L_β(inter) and disordered bilayer or L_α phase at approx. 41°C. The L_α phase had a bilayer repeat spacing of approx. 7.96 nm and a broad, diffuse acyl chain diffraction peak. The acyl chain diffraction peak was too broad and the intensity too low to accurately determine the repeat spacing but it was observed at approx. 0.47 nm which is consistent with previous values determined for the L_α acyl chain scattering peak [17]. This transformation proceeds via a two-state coexistence of initial and final phases (Figs. 2 and 5); or an apparent first-order thermodynamic process. The transition temperature is consistent with previous reports [13] although the L_α *d*-spacing is greater than previously reported [11]. It is clear from Fig. 1, however, that the system at no time transforms into the gel state rippled phase (P_β or $P_{\beta'}$). The presence of ripples would have been indicated by additional diffraction peaks due to the diagonals within the two-dimensional ripple phase unit cell [33]. Hatta and co-workers [34] as well as Wack and Webb [35] have recently indexed these reflections for DMPC and DPPC bilayers. This lack of a gel state ripple phase for DPPC in 1 M KSCN is consistent with previous observations for DPPC in ethanol/water solutions [4,14] which also induce only an interdigitated phase in the gel state, and thus may be common to all solvent induced interdigitated phases. These results are atypical of DHPC, an analogue of DPPC, in water [2,4] which naturally forms an interdigitated gel state bilayer that can transform during dynamic or equilibrium temperature changes into a $P_{\beta'}$ phase. It is apparent that the change in solvent structure at the bilayer-solvent interface is sufficient to change the packing of the lipid headgroups so that chain interdigitation from apposing leaflets within a bilayer occurs. We have previously speculated [24] that such a change in the solvent-bilayer interface structure is sufficient to allow the bilayer to produce mechanical stresses resulting from the thermally induced expansion of the headgroup area which are dissipated within the bilayer and/or solvent structure resulting in a preference for a gel bilayer phase with no need to form fluctuations within the bilayer and hence no eventual formation of the rippled phase. Cevc [31] has recently proposed that the ripple phase is formed when there are strong headgroup interactions at the bilayer/water interface and that the interdigitated phase is formed when the chain interactions are much stronger than headgroup interactions. The changes in the headgroup interactions for the solute-modified bilayers (i.e., DPPC in 1 M KSCN or 150 mg ethanol/ml water) cause an enhancement of the chain–chain interactions which preclude the bilayer from rippling/undulating under thermomechanical stress. It is conceivable that there are lipid systems in which the headgroup interactions and acyl chain interactions are of comparable strength. Under this condition it may be possible to induce a phase that is a combination of both the interdigitated and ripple phase (work in progress).

In order to probe the true mechanism of the L_c(inter) → L_β(inter) transformation, and to determine if a P_β phase can be induced over a somewhat longer temporal interval, a sample of DPPC in 1 M KSCN was examined while

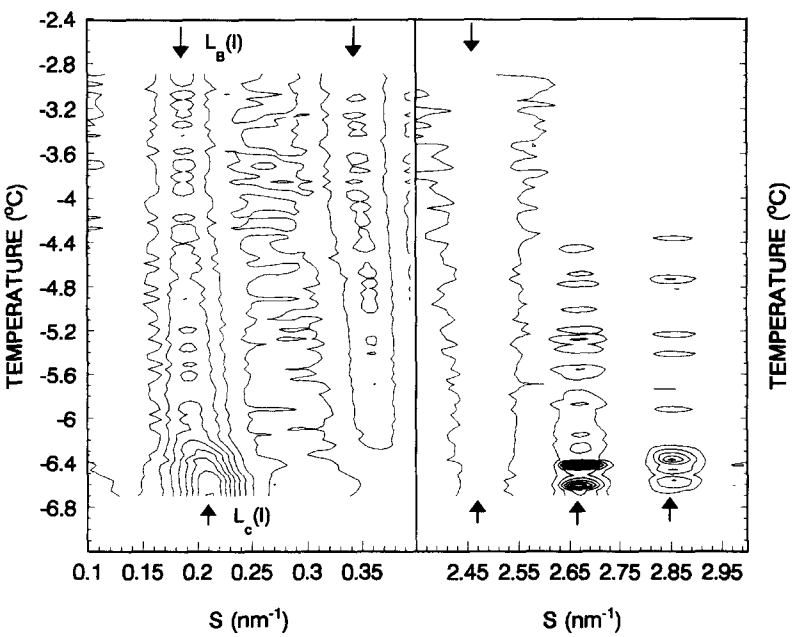

Fig. 7. Two-dimensional projection of the diffraction patterns from Fig. 6 for DPPC in 1 M KSCN undergoing a heating scan of 0.2°C/min. The characteristic diffraction maxima of the L_c(inter) and L_β(inter) are indicated by arrows in the small-angle region whereas the position of the diffraction maxima arising from the acyl chains are indicated by arrows in the wide-angle region.

undergoing a slow temperature scan of 0.2°C/min. Figs. 6 and 7 show representative X-ray patterns for DPPC in 1 M KSCN undergoing a slow scan through the L_c(inter) to L_β(inter) phase transition. It is clear from Fig. 7 that this transformation proceeds via a continuous or second order phase transition. Further collection of data (not shown) once again did not indicate the presence of the P_β phase intermediate between the L_β(inter) and L_α phases. In all cases, there is little difference between the structural and thermodynamic parameters determined for slow and fast scans in this system.

4. Conclusion

The phase structures and transitions for DPPC in 1 M KSCN have been determined using real-time X-ray diffraction and differential scanning calorimetry. In all cases, an interdigitated subgel bilayer phase was induced before characterization began. The L_c(inter) → L_β(inter) → L_α phase transition sequence was observed and characterized. Particular attention was paid to the transition mechanism between the L_c(inter) and L_β(inter) phases. It was found that this transition is similar to that involving non-interdigitated phases, namely, one of the axes of the rectangular subgel acyl chain unit cell expands until only one spacing is present indicating the foundation of an hexagonal acyl chain unit cell. Finally, a rippled bilayer phase was not seen as an intermediate between the gel bilayer (L_β(inter)) and disordered bilayer (L_α) states. In addition, we have speculated that the absence of a rippled phase indicates that the mechanical stress produced by the thermal expansion of the bilayer is absorbed by the lipid bilayer structure rather than being mechanically released via the introduction of undulations within the bilayer phase [4]. This absence of a ripple phase can be justified by Cevc's interaction theory [31].

Acknowledgements

This work was supported in part by Mount Sinai Hospital Service Club and by the VA Merit Review Board. We would like to thank Dr. Wim Bras and the staff of the Synchrotron Radiation Source, Daresbury Laboratory (U.K.) for assistance during these experiments.

References

[1] Ruocco, M.J., Siminovich, D.J. and Griffin, R.G. (1985) Biochemistry 24, 2406–2411.
[2] Laggner, P., Lohner, K., Degovics, G., Muller, K. and Schuster, A. (1987) Chem. Phys. Lipids 44,31–60.
[3] Kim, J.T., Mattai, J. and Shipley, G.G. (1989) Biochemistry 26, 6592–6598.
[4] Cunningham, B.A., Wolfe, D.H., Lis, L.J., Quinn, P.J., Collins, J.M., Tamura-Lis, W., Kucuk, O., Westerman, M.P. (1993) Mol. Cryst. Liq. Cryst. 225, 33–41.
[5] McDaniel, R.V., McIntosh, T.J. and Simon, S.A. (1983) Biochim. Biophys. Acta 731, 97–108.
[6] McIntosh, T.J., McDaniel, R.V. and Simon, S.A. (1983) Biochim. Biophys. Acta 731, 109–114.
[7] Rowe, E.S. (1983) Biochemistry 22, 3299–3305.
[8] Simon, S.A. and McIntosh, T.J. (1984) Biochim. Biophys. Acta 773, 169–172.
[9] O'Leary, T.J. and Levin, I.W. (1984) Biochim. Biophys. Acta 776, 185–189.
[10] Cunningham, B.A. and Lis, L.J. (1986) Biochim. Biophys. Acta 861, 237–242.
[11] Cunningham, B.A., Lis, L.J. and Quinn, P.J. (1986) Mol. Cryst. Liq. Cryst. 141, 361–367.
[12] Cunningham, B.A. and Lis, L.J. (1989) J. Colloid Interface Sci. 128, 15–25.
[13] Cunningham, B.A., Tamura-Lis, W., Lis, L.J. and Collins, J.M. (1989) Biochim. Biophys. Acta 984, 109–112.
[14] Tamura-Lis, W., Lis, L.J., Qadri, S. and Quinn. P.J. (1990) Mol. Cryst. Liq. Cryst. 178, 79–88.
[15] Lis, L.J. and Quinn, P.J. (1990) J. Appl. Crystallogr. 24, 48–60.
[16] Callen, H.B. (1960) Thermodynamics, Wiley, New York.
[17] Tenchov, B.G., Lis, L.J. and Quinn, P.J. (1987) Biochim. Biophys. Acta 897, 143–151.
[18] Lis, L.J., Tamura-Lis, W., Lim, T.K. and Quinn, P.J. (1990) Biochim. Biophys. Acta 1021, 201–204.
[19] Quinn, P.J. and Lis, L.J. (1987) J. Colloid Interface Sci. 115, 220–224.
[20] Lis, L.J. and Quinn, P.J. (1986) Mol. Cryst. Liq. Cryst. 140, 319–325.
[21] Quinn, P.J. and Lis, L.J. (1989) Mol. Cryst. Liq. Cryst. 167, 109–121.
[22] Lis, L.J., Tamura-Lis, W., Mastran, T., Patterson, D., Collins, J.M., Quinn, P.J. and Qadri, S. (1990) Mol. Cryst. Liq. Cryst. 178, 11–19.
[23] Tenchov, B.G., Yao, H. and Hatta, I. (1989) Biophys. J. 56, 757–768.
[24] Caffrey, M. (1984) Nucl. Instrum. Methods 222, 329–338.
[25] Gruner, S.M. (1987) Science 238, 305–312.
[26] Laggner, P. (1986) in Structural Biological Uses of X-ray Absorption, Scattering and Diffraction (Chance, B. and Bortnik, H.D., eds.), Academic Press, New York, pp. 171–182.
[27] Laggner, P., Lohner, K. and Muller, K. (1987) Mol. Cryst. Liq. Cryst. 151, 373–388.
[28] Laggner, P. (1988) Top. Curr. Chem. 245, 175–202.
[29] Baum, C.W. and Howells, E.B. (1954) Nature (London) 174, 549–551.
[30] Boulin, C., Kempf, R., Koch, M.H.J. and McLaughlin, S.M. (1986) Nucl. Instrum. Meth. Phys. Res. A249, 399–407.
[31] Cevc, G. (1991) Biochim. Biophys. Acta 1062, 59–69.
[32] Caffrey, M. (1987) Biochim. Biophys. Acta 896, 123–127.
[33] Quinn, P.J., Lis, L.J. and Cunningham, B.A. (1988) J. Colloid Interface Sci. 125, 437–443.
[34] Matuoka, S., Kato, S., Akiyama, M., Amemiya, Y. and Hatta, I. (1990) Biochim. Biophys. Acta 1028, 103–109.
[35] Wack, D.C. and Webb, W.W. (1989) Phys. Rev. A40, 2712–2730.